

Electrochemical Behaviour of Nanoscale Ni Modified Screen-Printed Carbon Electrodes in Corrosion Tests and Hydrogen Evolution Electrocatalysis

Lenka Škantárová^{1,*}, Renáta Oriňaková¹, Andrea Straková Fedorková¹, Petr Bača², Marie Sedlaříková², Andrej Oriňak¹

¹ Department of Physical Chemistry, Faculty of Natural Sciences, Pavol Jozef Šafárik University, Moyzesova 11, 040 01 Košice, Slovak Republic;

² Department of Electrical and Electronic Technology, Faculty of Electrical Engineering and Communication, Brno University of Technology, Technická 10, CZ-61600 Brno, Czech Republic;

*E-mail: lenka.skantarova@upjs.sk

Received: 15 May 2015 / Accepted: 12 June 2015 / Published: 26 August 2015

Corrosion resistance and electrocatalytic activity were examined for nickel nanoparticles (NiNPs) coated screen-printed carbon-based electrodes (SPCEs) being a novel alternative to unmodified electrodes. The electrodeposition was used as a cost-efficient and time-saving method for preparation of NiNPs-SPCEs. NiNPs were characterized by scanning electron microscopy (SEM). Corrosion as well as hydrogen evolution reaction (HER) measurements were performed in 1 mol/L H₂SO₄ using potentiodynamic polarization method, moreover electrochemical impedance spectroscopy (EIS) experiments were carried out. The kinetic parameters were determined from corrosion tests and equilibrium potential values from HER. Presented current state-of-the-art focuses on the functional NiNPs catalyzator preparation opening the way to rapid 'in-situ' analyses in sensing applications.

Keywords: nickel; EIS; acid corrosion; anodic dissolution; electrodeposited films; hydrogen evolution; screen-printed electrodes (SPEs)

1. INTRODUCTION

Nanocrystalline materials are the main subject of interest in commercial applications due to their unusual properties [1]. At a microscopic level, the existence of pores, crevices, microcavities, etc. favors the increase of the electrode surface area, although mass transfer, ohmic and bubble overvoltages prevent the rates of electrochemical reactions from increasing proportionally. At nanoscopic levels, a change in the superficial ordering of the metal atoms can have a significant effect

on the kinetics of reactions involving adsorbed intermediates [2]. Comprehensive understanding of the relation between corrosion properties of the nanocrystalline materials and their structure is important both for following applications as well as to understand their fundamental physical/chemical properties [3].

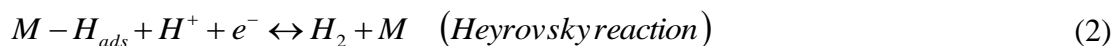
Corrosion behaviour of nanocrystalline metals varies depending on their nanostructure parameters, e. g. grain size. In an effort to achieve nanoscale Ni grain size the appropriate agents like saccharine and sodium citrate are added to working electrolytes used in electrodeposition preparation process [4, 5]. Nickel and nickel alloys can be used in electroanalysis and electrocatalysis requiring corrosion and heat resistance. The resulting nickel deposits exhibit low internal stress and good ductility. Simple preparation, electroinactivity in physiological solutions and high porosity are additional advantages of nickel oxide nanomaterials for biomolecules encapsulation [6].

Screen-printing is one of the most promising approaches towards simple, fast and cost-efficient production of biosensors. Disposable sensors in pursuance of screen printed electrodes (SPEs) including microelectrodes and modified electrodes have led to new possibilities in the detection and quantitation of biomolecules, pesticides, antigens, DNA, microorganisms and enzymes. SPE-based sensors are in line with the growing need for performing rapid and accurate “in situ” analyses and for the development of portable devices. In fact, interest in the fabrication of biosensors with high sensitivity, selectivity and efficiency is rapidly growing [7-13]. The preparation of nanoparticle-modified electrodes includes the synthesis of nanoparticles and attachment of the nanomaterials to electrodes. Therefore, it is necessary to investigate the different nanosize electrode materials as well as the novel attachment approaches applying in electrochemical sensors [14-16].

In acidic solutions; nickel is capable of passivating to a considerable extent. This is a feature not predicted by the potential-pH equilibrium diagram and it is one of the reasons why in practice, corrosion resistance of nickel in acid solutions is better than that predicted from considerations of thermodynamic equilibria [17]. Nanoscale Ni grains exhibited higher passive current densities values during active-passive electrochemical polarization behaviour relative to polycrystalline nickel [5, 18].

Electrochemical impedance spectroscopy (EIS) has been widely used for studying the electrochemical mechanisms occurring on the electrodes. EIS is a good tool for the analysis of the kinetics of electrode reactions. The various elements in this equivalent circuit are related to the metal/film and film/solution interfaces and the phenomena occurring inside the passive film. EIS measurements make it possible to obtain some information on the mechanism, establishing a theoretical transfer function and developing the passive film growth model [19-21].

The hydrogen evolution reaction (HER) is very significant and has been broadly studied using a wide range of media, and electrode materials [22, 23]. It is well established that the HER on a metallic electrode M, in acidic solution, proceeds according to the subsequent reaction mechanism:



The goal of this work was to investigate the electrochemical corrosion behaviour of nickel NPs-SPCE in acidic solution. We also report the study of the current-potential dependence for HER on electrodeposited nickel as a low cost electrocatalyst in sulphuric acid solution. The influence of different NiNPs electrodeposition times on electrochemical corrosion parameters and enhanced activity in HER was examined. The electrocatalytic characteristics of Ni nanoparticles modified SPCEs play very important role for their prospective use in miniaturized total-analysis systems and sensing applications for sensitive biomolecules electrochemical detection.

2. EXPERIMENTAL SECTION

2.1. Apparatus and Electrodes

The electrodeposition process, corrosion tests, electrochemical impedance spectroscopy measurements and hydrogen evolution reaction studies were performed with the same electrochemical cell at room temperature and at atmospheric pressure. The electrochemical measurements were carried out with screen-printed carbon electrode system consisting of three electrodes: graphite working electrode (diameter 4.0 mm), Ag/AgCl reference electrode and graphite counter electrode. A three-electrode SPCE system was fabricated with a semi-automatic screen-printing machine DEK 248 (DEK International, Switzerland). The inks used for this process were: Autostat HT5 polyester sheet (McDermid Autotype, UK), Electrodag 423SS carbon ink, Electrodag 6037SS silver/silver chloride ink and Minico 7000 Blue insulating ink (Acheson Industries, The Netherlands).

The electrochemical measurements were conducted using an Autolab PGSTAT 302N potentiostat/galvanostat connected to a PC and controlled by Autolab Nova software. All measurements were performed with a working electrolyte volume of 50 μL , which was enough to cover the three-electrode system connected to the potentiostat by a small connector. The morphology and homogeneity of nanoscale Ni modified SPCEs were examined by a scanning electron microscope (JOEL JSM-7001F, Japan). All experiments were repeated and good reproducibility was obtained.

2.2. Reagents and Solutions

All used chemicals (boric acid, $\text{NiSO}_4 \cdot 6\text{H}_2\text{O}$, $\text{NiCl}_2 \cdot 6\text{H}_2\text{O}$, H_3BO_3 , sodium citrate, sulphuric acid) were purchased from REACHEM or Laboratory Chemicals - Milan Adamík (Slovakia) and were of the highest grade available and used without other purification.

2.3. SPCEs Surface Modification with NiNPs

The solution, in which the nickel deposition was carried out, typically consisted of 0.7 mol/L $\text{NiSO}_4 \cdot 6\text{H}_2\text{O}$, 0.6 mol/L $\text{NiCl}_2 \cdot 6\text{H}_2\text{O}$, 0.6 mol/L H_3BO_3 and 0.05 mol/L sodium citrate. The electrochemical synthesis of metallic nickel was performed using a constant potential value of -2.0 V

in a working electrolyte containing the nickel sulphate, with the deposition times of 5 s, 10 s, 30 s, 50 s, 70 s and 90 s.

2.4. Electrochemical Study of NiNPs Modified SPCEs Corrosion Behaviour and Electrocatalytic Activity

Before corrosion and HER electrochemical measurements, the samples were dipped in electrolyte for 120 s for stabilization of the open circuit potential (OCP). Corrosion tests for nickel nanoparticles substrates were performed in a 1 mol/L sulphuric acid solution. The anodic polarization curves were obtained in the potential range from -0.6 V to +0.1 V at a scanning rate of 0.5 mV/s. Corrosion current density, potential and rate were obtained using the Tafel extrapolation method.

For the corrosion study, polarization resistances can be also evaluated from electrochemical impedance spectroscopy data (EIS). The potentiostat is controlled via a PC which also captures the EIS data. The applied frequency was varied from 10 kHz to 0.01 Hz. The electrical model that we used to simulate this type of electrochemical behaviour is given in Figure 1. A similar equivalent circuit model was earlier applied by Das and Sahoo [24].

The charge transfer resistance (R_{ct}) was represented by the resistance of electron transfer during electrochemical reaction course. The double layer capacitance (C_{dl}) can be correlated to the delamination of the coating. Solution resistance (R_s) was referred to the resistance between the working electrode and reference electrode. The values of charge transfer resistance and double layer capacitance were determined from the Nyquist plot by fitting a semicircle using the instruments software.

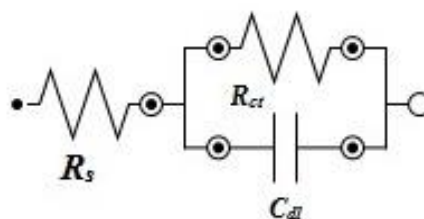


Figure 1. Equivalent circuit used to fit EIS data.

The HER activity of resulting NiNPs modified SPCEs was also evaluated in 1 mol/L H_2SO_4 solution applying a slow potentiodynamic sweep of 0.5 mV/s in the range of potentials from 0 V to -1 V. In the case of Ni nanoparticles electrodeposited after 5 s and 10 s, the potential range was shifted from +0.2 V to -0.7 V. For the reduction of nickel oxides on the electrocatalytic layer, the NiNPs modified SPCEs were polarized in 1 mol/L H_2SO_4 at -500 mV for 180 s before hydrogen evolution measurement.

3. RESULTS AND DISCUSSION

The aim of actual study was to investigate the influence of NiNPs electrodeposition time that correlated with NiNPs resulting size on their corrosion stability and electrocatalytic activity in sulphuric acid as a test solution.

3.1. Microscopic Characterization of NiNPs Modified SPCEs

The obtained electrodeposited NiNPs on SPCEs were studied by SEM at different magnifications. The choice of optimal magnification is important to obtain images that show agglomeration of nanoparticles in the electrodeposited layers. The size of electrochemically synthesized nanoparticles depends on the period of deposition process. The SEM analysis primarily targeted surface morphology and homogeneity of electrodeposited nickel nanoparticles. In Figure 2 the selected SEM micrographs of Ni nanoparticles modified SPCEs are displayed for different deposition periods of 5 s, 10 s, 50 s and 70 s. Particles deposited during period 30 s and 90 s were similar to the particles deposited during period 50 and 70 s therefore, are not shown.

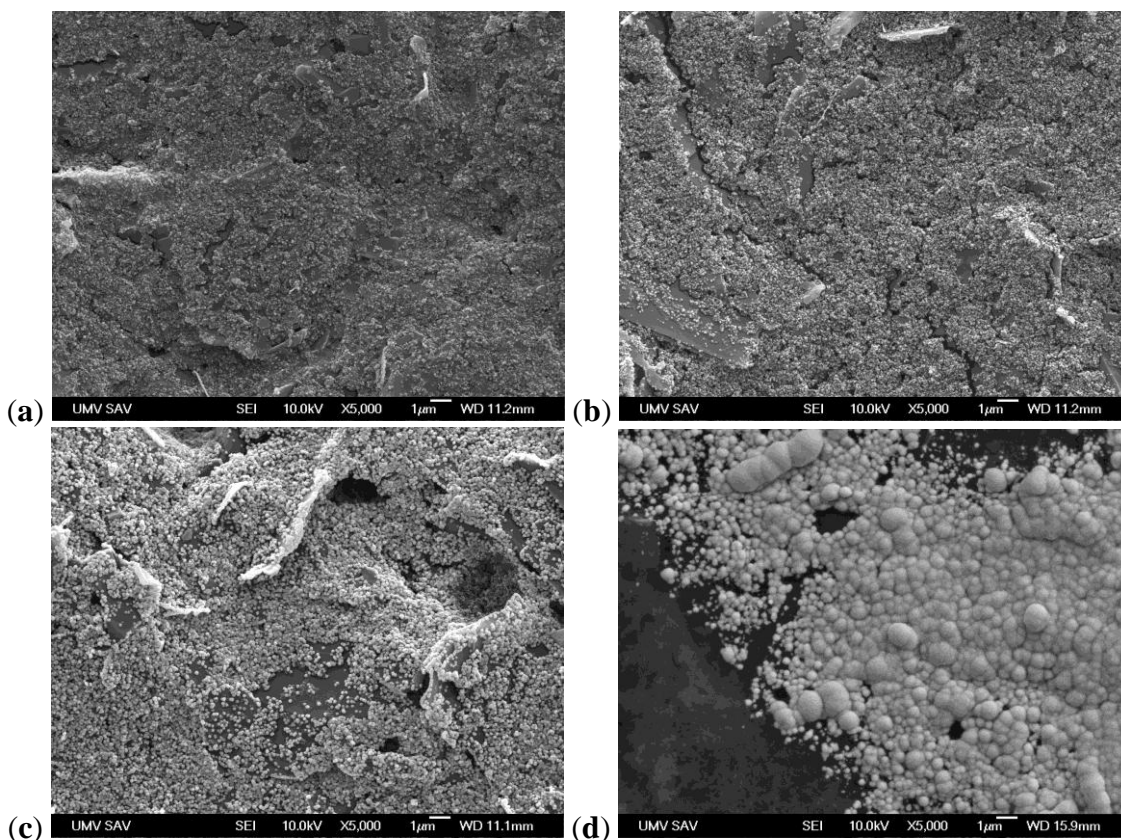


Figure 2. Representative SEM images of NiNPs electrodeposited onto SPCEs using deposition period of (a) 5 s; (b) 10 s; (c) 50 s and (d) 70 s.

The surface of SPCE working electrode was covered with Ni nanoparticles with different size distribution. A similar, oval-shaped nickel nanoparticles about 20 nm in diameter, were homogeneously distributed onto SPCE after 5 s (see Figure 2a). As follows from Figure 2a, there was a reduced coverage of SPCE with Ni nanoparticles at this deposition time. Further it is clear, that we observed the increase in both the size (from ca. 80 nm to 250 nm in diameter) and density of NiNPs with increasing electrodeposition time of 10 s, 30 s and 50 s (Figure 2b, Figure 2c). With the additional increase of deposition time, Ni nanoparticles also became more aggregated. Ni nanoparticles electrochemically synthesized after 70 s and 90 s (Figure 2d) showed the highest size (from ca. 250 nm to 900 nm) and coverage of working electrode.

3.2. Electrochemical Corrosion Behaviour of NiNPs Modified SPCEs

Electrochemical stability of electrodeposited nanocrystalline nickel particles was studied by anodic polarization curves at room temperature. The representative Tafel plots obtained for NiNPs modified SPCEs in sulphuric acid solution are shown in Figure 3. The reproducibility of potentiodynamic polarization curves was very good. NiNPs on SPCE were still observed by SEM after anodic dissolution process. We observed active-passive behaviour for NiNPs modified SPCEs in all polarization curves. Passivation behaviour of all samples was noticed at a more positive potential values than corrosion potential values. A zero current potential shift towards the more positive values with decreasing NiNPs size was observed. The increase of NiNPs electrodeposition time resulted in a shift of corrosion potential to more negative values with an associated increase of corrosion rate.

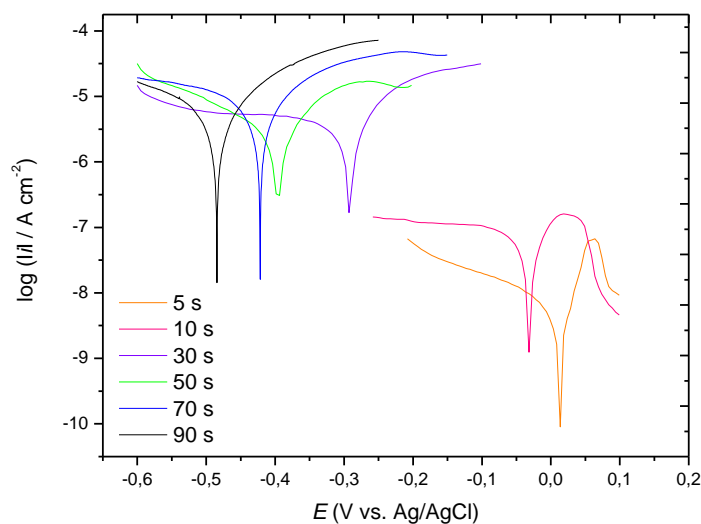


Figure 3. Representative details of potentiodynamic polarization curves of NiNPs modified SPCEs in 1 mol/L H_2SO_4 solution at room temperature.

The electrochemical kinetic parameters such as corrosion potential (E_{corr}) and corrosion current density (i_{corr}) were determined from the intersection of the anodic and cathodic Tafel lines extrapolation. The corresponding numerical values of corrosion current density, corrosion potential and corrosion rate are summarized in Table 1.

Table 1. Determined values of E_{corr} , i_{corr} , corrosion rates and Tafel slopes obtained from potentiodynamic polarization curves of NiNPs modified SPCEs in 1 mol/L H_2SO_4 solution at room temperature.

NiNPs deposition time (s)	E_{corr} (mV)	i_{corr} ($\mu A/cm^2$)	Corrosion rate (mm/year)	b_a (mV/dec)
5	+14.0	2.779×10^{-2}	4.057×10^{-6}	60
10	-35.2	4.354×10^{-2}	6.355×10^{-6}	78
30	-291	3.464	5.056×10^{-3}	105
50	-390	15.23	2.223×10^{-2}	123
70	-421	11.60	1.693×10^{-2}	160
90	-485	7.341	1.072×10^{-2}	170

The resulting Tafel plots displayed the highest corrosive resistance for Ni nanoparticles electrolytically synthesized using the 5 s time interval. A significant decrease of corrosion potential at value of -291 mV was observed for NiNPs sample deposited after 30 s. Furthermore, the Tafel curves indicated the increase of corrosion current density with increasing NiNPs electrodeposition time and associated increase of Ni particles size. Tafel slopes values (b_a) corresponding to anodic corrosion dissolution process increased with time of electrodeposition (Table 1). This behavior is contributed to the faster corrosion process of bigger Ni nanoparticles. Ni nanoparticles with smaller diameter are passivated with homogeneous layer and therefore the smallest NiNPs exhibited the lowest corrosion rate. The corrosion rate of our six samples was evaluated to be between 4.057×10^{-6} and 1.072×10^{-2} mm/year. This investigation is consistent with the research performed by Li-yuan [1] and Mishra et al. [5]. In the case of nickel nanoparticles electrodeposited using 90 s we noticed corrosion potential value of -485 mV, meaning that these nanoparticles were less resistant. Potentiodynamic polarization curves demonstrated a shift of corrosion potential to more negative values and a decrease in electrochemical stability with increasing Ni particles size. The best electrochemical stability in corrosive aqueous media and the highest corrosion potential of +14.0 mV was displayed by NiNPs electrodeposited onto SPCE after a period of 5 s. Decrease of corrosion rate values together with decreasing NiNPs size indicated greater hindrance to anodic dissolution in nanoscale Ni modified SPCEs.

3.3. Electrochemical Impedance Spectroscopy Measurements of NiNPs Modified SPCEs

The EIS technique has proven to be a valuable test tool for the electrochemical characterization of the protective films on metals. This method provides detailed data on the effectiveness of a film over a relatively small area [19].

Thus, the EIS technique was chosen to characterize the corrosion behaviour of NiNPs in the present study. We used the electrical circuit model given in Figure 1 for simulating electrochemical behaviour of the NiNPs coated SPCEs. Nyquist plots obtained from the tests in general exhibited a single semicircle in the high frequency region which is quite consistent to that observed by Narayanan et al. [25]. The Nyquist impedance plots obtained from the corrosion tests in an acidic media of 1 mol/L H_2SO_4 for NiNPs electrolytically synthesized using six various deposition times onto SPCEs can be seen in Figure 4a. A detailed view of Nyquist diagrams observed for three highest electrodeposition periods is shown in Figure 4b.

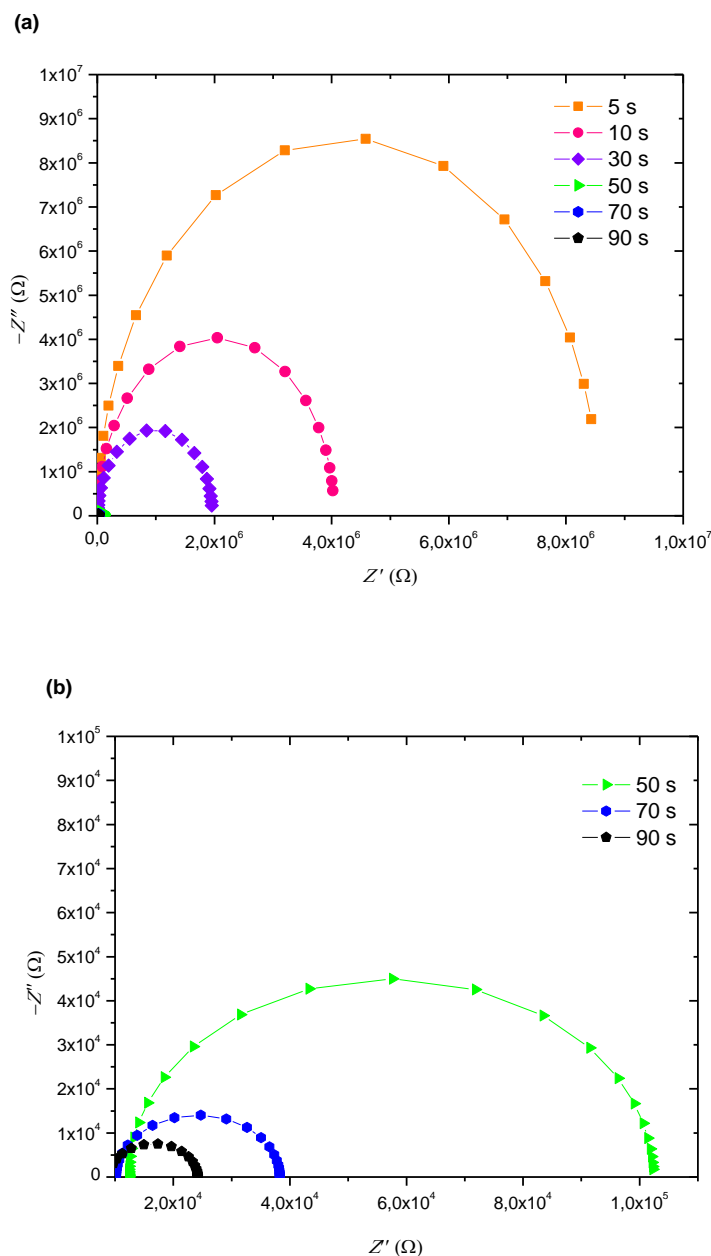


Figure 4. (a) Representation of Electrochemical Impedance Spectroscopy (Nyquist diagrams) for the NiNPs-SPCEs (six deposition periods in 1 mol/L H_2SO_4). (b) Detail of Nyquist plots for NiNPs prepared using different deposition time of 50 s; 70 s; 90 s.

Table 2 contains the values of solution resistance (R_s), charge transfer resistance (R_{ct}), double layer capacitance (C_{dl}) as obtained from the Nyquist impedance plots by fitting a semicircle using the instruments software.

Table 2. Equivalent circuit parameters determined by modelling impedance spectra of Ni nanoparticles modified SPCEs with different NiNPs deposition period in 1 mol/L H_2SO_4 at room temperature. Estimated error took values between 0.18% and 1.6%. Surface area of working SPE electrode was 0.126 cm^2 .

NiNPs deposition period (s)	R_s (Ω)	R_{ct} (Ω)	C_{dl} (F)
5	9426.8	8.5646×10^6	2.412×10^{-7}
10	10524	4.0318×10^6	2.805×10^{-7}
30	9488.4	1.9527×10^6	4.899×10^{-7}
50	12349	89954	3.394×10^{-6}
70	10181	28099	2.041×10^{-6}
90	9100.9	15073	1.847×10^{-6}

For all samples we observed approximately comparable values of solution resistance (R_s). At shorter deposition periods of 5 s; 10 s; 30 s small separated Ni nanoparticles were formed and these samples demonstrated higher resistance. A decrease of charge transfer resistance (R_{ct}) for our NiNPs-SPCEs samples with increasing deposition period was observed. This conclusion confirmed improved electron transfer for this reaction for the NiNPs prepared at higher deposition period. The lower values of resistance are associated with higher amount of electrochemically active sites for the HER. With increasing electrodeposition time there was a tendency of NiNPs to form agglomerates with a simultaneous creation of a more coherent metallic film on the surface of working electrode. C_{dl} element is used to fit the data of the interface between an electrode and the electrolyte. The values of double layer capacitance (C_{dl}) (Table 2) increased with increasing NiNPs deposition time. The increasing values of C_{dl} indicated the increasing roughness of the NiNP modified SPCEs with increasing deposition time. After fitting of the measured data, the estimated error took values between 0.18% and 1.6%.

3.4. Electrocatalytic Activity of NiNPs Modified SPCEs

The HER activity of NiNPs-SPCEs was evaluated depending on electrodeposition time and the size of NiNPs at room temperature. All the curves were similar and the representative current versus potential plots recorded during HER in 1 mol/L H_2SO_4 solution are given in Figure 5. The results were obtained by applying a slow potentiodynamic sweep of 0.5 mV/s in the range of potentials from 0.2 V to -0.7 V. The linear cathodic regions of the Tafel plots indicate that the HER on NiNPs modified SPCEs is kinetically controlled by charge transfer. It is clearly seen, that there was an equilibrium potential shift to more negative potential values ($-4.00\text{ mV} \rightarrow -304\text{ mV}$) with increasing

electrodeposition time and corresponding size of Ni nanoparticles. Smaller Ni nanocrystalline particles in general offered higher electrocatalytic activity in HER compared to bigger aggregated Ni particles.

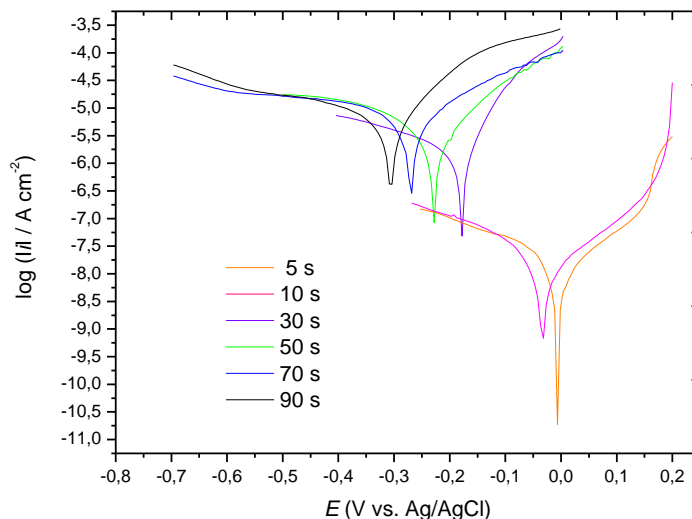


Figure 5. Dependence of the logarithm of the current density on potential for HER in 1 mol/L H_2SO_4 solution at room temperature for NiNPs modified SPCEs.

The best catalytic activity was detected for NiNPs prepared with electrodeposition period of 5 s. The lowest Tafel slope of 57 was also obtained for this sample. Tafel slopes of the other samples were between 57 mV and 117 mV (Table 3).

Table 3. Determined values of equilibrium potentials and cathodic Tafel slopes on NiNPs modified SPCEs in 1 mol/L H_2SO_4 solution at room temperature.

NiNPs deposition time (s)	E_{eq} (mV)	b_c (mV/dec)
5	-4.00	57
10	-33.0	60
30	-183	99
50	-230	85
70	-272	109
90	-304	117

There was observed a shift of equilibrium potential towards noble direction for smaller nanoscale Ni particles beside bigger NiNPs. According to the general model of the HER mechanism, Volmer reaction (Equation 1) is rate determining step on NiNP modified SPCEs, with Tafel slope value of 116-120 mV/dec.

4. CONCLUSIONS

In an effort to develop metal nanoparticles with corrosion stability and enhanced electrocatalytic activity we prepared NiNPs modified SPCEs by electrodeposition process. The resulting Ni nanoparticles structure was characterized by scanning electron microscope. We subsequently studied corrosion and also electrocatalytic properties for hydrogen evolution reaction (HER) in 1 mol/L H₂SO₄ using potentiodynamic polarization method. Nickel modified SPCEs exhibited active-passive polarization behaviour in corrosion tests. Corrosion behaviour of NiNPs-SPCEs was strongly affected by nanoparticles size. We observed lower corrosion rates for smaller NiNPs as compared to Ni aggregates. In the case of bigger and aggregated Ni particles corrosion potential values were shifted to more negative values. HER measurements showed a potential shift to more negative equilibrium potential values with the increase of NiNPs deposition time associated with a Ni particles size growth. The best electrochemical corrosion resistance and the highest activity in HER was registered for Ni nanoparticles deposited using 5 s. Combination of electrochemical screen-printed sensors with active and stable nanoscale Ni particles and films presents a considerable step towards improved sensitivity, long-term stability of the bioelements in sensors and novel detection options for these disposable microanalytical devices.

ACKNOWLEDGMENTS

This research work has been carried out in the Centre for Research and Utilization of Renewable Energy (CVVOZE). Authors gratefully acknowledge financial support from the Ministry of Education, Youth and Sports of the Czech Republic under NPU I programme (project No. LO1210). The authors would like to acknowledge the financial support by VVGS-2014-187. We would like to thank ICN2 (Spain) for providing of screen-printed electrodes.

References

1. Q. Li-yuan, L. Jian-she and J. Qing, *Trans. Nonferrous Met. Soc. China*, 20 (2010) 82.
2. C.A. Marozzi and A.C. Chialvo, *Electrochim. Acta*, 45 (2000) 2111.
3. K. Lu, *Mater. Sci. Eng. R-Rep.*, 16 (1996) 161.
4. M. Abraham, P. Holdway, M. Thuvander, A. Carezo and G.D.W. Smith, *Surf. Eng.*, 18 (2002) 151.
5. R. Mishra and R. Balasubramaniam, *Corros. Sci.*, 46 (2004) 3019.
6. A. Salimi, A. Noorbakhsh and A.J. Semnani, *Solid State Electrochem.*, 15 (2011) 2041.
7. Z. Taleat, A. Khoshroo and M. Mazloum-Ardakani, *Microchim. Acta*, 181 (2014) 865.
8. M. Boujtita, J.P. Hart and R. Pittson, *Biosens. Bioelectron.*, 15 (2000) 257.
9. J.D. Newman, A.P.F. Turner and G. Marrazza, *Anal. Chim. Acta*, 262 (1992) 13.
10. J.D. Newman and S.J. Setford, *Mol. Biotechnol.*, 32 (2006) 249.
11. R. Foster, J. Cassidy and E. O'Donoghue, *Electroanal.*, 12 (2000) 716.
12. B.B. Rodriguez, J.A. Bolbot and I.E. Tothill, *Anal. Bioanal. Chem.*, 380 (2004) 284.
13. L. Tymecki, E. Zwierkowska and R. Koncki, *Anal. Chim. Acta*, 538 (2005) 251.
14. S. Marín and A. Merkoçi, *Electroanal.*, 24 (2012) 459.
15. J. Lin, M.D. Zhou, S.B. Hočevár, E.T. McAdams, B. Ogorevc and X. Zhang, *Front. Biosci.*, 10 (2005) 483.
16. O. Domínguez Renedo, M.A. Alonso-Lomillo and M.J. Arcos Martínez, *Talanta*, 73 (2007) 202.

17. K.F. Khaled, *Electrochim. Acta*, 55 (2010) 5375.
18. R. Rofagha, R. Langer, A.M. El-Sherik, U. Erb, G. Palumbo and K.T. Aust, *Scripta Metall. Mater.*, 25 (1991) 2867.
19. E.B. Castro and J.R. Vilche, *Electrochim. Acta*, 38 (1993) 1567.
20. M. Jafarian, M. Behazin, I. Danaee and F. Gobal, *Res. J. Chem. Sci.*, 3 (2013) 56.
21. M. Gaberšček and M.S. Pejovnik, *Electrochim. Acta*, 41 (1996) 1137.
22. E. Navarro-Flores, Z. Chong and S. Omanovic, *J. Mol. Catal. A: Chem.*, 226 (2005) 180.
23. E.G. Badea, I. Maior, A. Cojocar and I. Corbu, *Rev. Roum. Chim.*, 52 (2007) 1123.
24. S.K. Das and P. Sahoo, *Portugaliae Electrochim. Acta*, 29 (2011) 211.
25. T.S.N.S. Narayanan and S.K. Seshadri, *J. Alloys. Compd.*, 365 (2004) 197.

© 2015 The Authors. Published by ESG (www.electrochemsci.org). This article is an open access article distributed under the terms and conditions of the Creative Commons Attribution license (<http://creativecommons.org/licenses/by/4.0/>).